ELSEVIER

Biochimica et Biophysica Acta 1412 (1999) 262–272

BIOCHIMICA ET BIOPHYSICA ACTA
BBA

www.elsevier.com/locate/bba

Voltammetric studies of bidirectional catalytic electron transport in *Escherichia coli* succinate dehydrogenase: comparison with the enzyme from beef heart mitochondria

Harsh R. Pershad [a], Judy Hirst [a], Bruce Cochran [b], Brian A.C. Ackrell [b], Fraser A. Armstrong [a,*]

[a] *Inorganic Chemistry Laboratory, University of Oxford, South Parks Road, Oxford OX1 3QR, UK*
[b] *Department of Biochemistry and Biophysics, VA Medical Center Molecular Biology Division, University of California, San Francisco, CA 94121, USA*

Received 17 February 1999; received in revised form 28 April 1999; accepted 3 June 1999

Abstract

The succinate dehydrogenases (SDH: soluble, membrane-extrinsic subunits of succinate:quinone oxidoreductases) from *Escherichia coli* and beef heart mitochondria each adsorb at a pyrolytic graphite 'edge' electrode and catalyse the interconversion of succinate and fumarate according to the electrochemical potential that is applied. *E. coli* and beef heart mitochondrial SDH share only ca. 50% homology, yet the steady-state catalytic activities, when measured over a continuous potential range, display very similar catalytic operating potentials and energetic biases (the relative ability to catalyse succinate oxidation vs. fumarate reduction). Importantly, *E. coli* SDH also exhibits the interesting 'tunnel-diode' behaviour previously reported for the mitochondrial enzyme. Thus as the potential is lowered below ca. −60 mV (pH 7, 38°C) the rate of catalytic fumarate reduction decreases abruptly despite an increase in driving force. Since the homology relates primarily to residues associated with active site regions, the marked similarity in the voltammetry reaffirms our previous conclusions that the tunnel-diode behaviour is a characteristic property of the enzyme active site. Thus, succinate dehydrogenase is an excellent fumarate reductase, but its activity in this direction is limited to a very specific range of potential.

1. Introduction

Succinate:ubiquinone oxidoreductase (SQR; EC 1.3.99.1) also known in mitochondria as 'Complex II', plays a central role in the energy production of aerobically respiring organisms, providing a link between the citric acid cycle and the membrane-bound electron-transport (oxidative phosphorylation) system. The membrane-extrinsic, water-soluble domain of SQR, known as succinate dehydrogenase (SDH), contains a 70-kDa 'Fp' subunit, housing the fumarate/succinate active site and a covalently bound $FAD/FADH_2$ group, and a smaller (27-kDa) 'Ip' subunit, which contains three iron–sulfur clusters (S1, $[2Fe–2S]^{2+/1+}$; S2, $[4Fe–4S]^{2+/1+}$; and S3, $[3Fe–4S]^{1+/0}$) (for reviews see [1–3]). Reduction potentials as measured by EPR spectroscopy for beef heart SQR and the corresponding enzyme from *Escherichia coli* are listed in Table 1 [4–7]. The interconversion of succinate and fumarate involves elec-

* Corresponding author. Fax: +44-1865-272690; E-mail: fraser.armstrong@chem.ox.ac.uk

0005-2728/99/$ – see front matter
PII: S0005-2728(99)00066-3

Table 1
Comparison of reduction potentials (mV vs. SHE) for the FAD (pH 7.0) and Fe–S clusters (pH 7.4) for SQR from beef heart and *E. coli*, as measured by EPR spectroscopy, with $\varepsilon_{F/S}$, ε_{cat} and ε_{switch} (pH 7.0, 38°C) obtained in the present electrochemical study

Redox couple	Beef heart SDH	*E. coli* SDH	ne^-/mH^+
$FAD/FADH_2$	−79 [4]	n.d.	$2e^-/2H^+$
S1 $[2Fe–2S]^{2+/1+}$	0 ± 15 [5]	+10 ± 20 [7]	$1e^-$
S2 $[4Fe–4S]^{2+/1+}$	−260 [5]	−175 ± 20 [7]	$1e^-$
S3 $[3Fe–4S]^{1+/0}$	+60 ± 15[6]	+65 ± 15 [7]	$1e^-$
$\varepsilon_{F/S}$	0 ± 15	0 ± 15	$2e^-/2H^+$
ε_{cat}	−35 ± 15	−35 ± 15	$1e^-$
ε_{switch}	−100 ± 15	−100 ± 15	$2e^-/2H+$

Estimated one-electron reduction potentials for the FAD group in beef heart SQR are E ($FADH^{\bullet}/FADH_2$) = −127 mV (pK = 8.0) and E ($FADH^{\bullet}/FADH_2$) = −31 mV (pK = 7.7) [4]; n.d. = as far as we are aware, the reduction potential for *E. coli* FAD has not been determined.

tron and proton transfer according to Eq. 1 [8]; in vivo the electrons are drawn from or donated to the membrane quinone pool.

$$\text{Fumarate} + 2e^- + 2H^+ \Leftrightarrow \text{Succinate}$$

$$E^{0'} = 0 \text{ to } +30 \text{ mV vs. SHE, pH 7.0, } 37°C \quad (1)$$

Previously, we studied the catalytic electron-transport properties of beef heart mitochondrial SDH using protein film voltammetry (PFV) [9–11]. In PFV, a redox protein or enzyme is adsorbed on an electrode surface, and 'interrogated' electrochemically, revealing a variety of redox and catalytic properties that are often not visible from conventional methods [12–14]. Requirements are: (a) that interfacial electron exchange is facile and the kinetics do not control the response; and (b) that there is retention of the enzyme's native properties (i.e. as might be measured in conventional solution experiments and would presumably prevail in vivo). PFV can provide important alternative perspectives on the operation of biological redox systems. If an active film contains sufficient molecules (up to monolayer coverage), diagnostic signals consisting of pairs of oxidation and reduction current peaks, due to reversible electron exchange with individual redox-active sites, may be visible. When these sites interact with species contained in the contacting electrolyte, the signals may shift or distort, while addition of a substrate transforms them to catalytic waves [12]. Since current is a direct measure of turnover, such catalytic waves reveal the potential (i.e. driving force) dependence of catalysis. Even if electroactive coverages are too low to permit observation of non-turnover signals, it is still possible to gain important information about catalytic electron transport. Redox-active sites are subjected to precise potential control across a wide and continuously variable potential range, the bias that enzymes possess to favour a particular redox direction can be quantified, and subtle effects, such as the presence of redox-state-dependent switches detected [9–19].

Interesting catalytic properties are indeed observed when SDH from beef heart mitochondria is adsorbed from dilute solution at a pyrolytic graphite 'edge' (PGE) electrode. If succinate and fumarate are both present, bidirectional catalysis is observed, the overall direction depending only on the potential that is applied [9–11]. Although the nature of the enzyme–electrode interaction is not clear, the adsorbed enzyme is clearly active and exchanges electrons freely with the electrode. It is also apparent that activity in the direction of fumarate reduction is very significant, but only within a narrow region of potential where the driving force is small. The results suggest that SQR itself should be able to catalyse effectively in the direction of fumarate reduction (i.e. as would reverse the oxidative citric acid cycle). This is consistent with the observations of Maklashina et al. [20] who expressed SQR in *E. coli* under anaerobic conditions, and showed that it catalyses a viable electron transport reaction between menaquinol and fumarate when the latter is the sole available electron acceptor.

Upon lowering the electrode potential past a certain critical value, ε_{peak}, the rate of fumarate reduction decreases abruptly [9–11]. Although the overall response is weaker, an identical catalytic profile, with the same value of ε_{peak}, was obtained at a gold electrode (a surface having significantly different interfacial characteristics) [21]. This phenomenon was termed the 'tunnel-diode' effect following the terminology for an electronic device which displays a region of negative resistance (the current decreases as the driving force is raised) [9]. Conventional solution-phase activity studies using reduced benzylviologen

as electron donor confirmed that, for SQR from various sources (beef heart, rat liver, human placenta, *Ascaris suum* and *E. coli*), the rate of fumarate reduction (monitored spectrophotometrically, not electrochemically) accelerates as the benzylviologen is consumed (and the driving force decreases). By contrast, for SQR from *Bacillus subtilis* and the established fumarate reductases from *E. coli* and yeast, normal behaviour was observed, the rate of fumarate reduction decreasing as the assay progressed [21]. The tunnel-diode effect has been suggested to be due to the reduced form of the active-site flavin moiety preferring a different conformation, which is less active in catalysis [10]. Further indication that it does not result instead from a change in the interaction between the enzyme and the electrode comes from the electrocatalytic responses of other enzymes, notably the fumarate reductases from *E. coli* [12,15,18] and *Shewanella frigidimarina* [19] which show normal behaviour (no evidence for any discontinuity as the potential is varied) on PGE electrodes in the same potential region (−0.2 to +0.1 V).

In order to clarify and investigate further the tunnel-diode effect, we have now studied the SDH from *E. coli*. This is a very similar to the beef heart enzyme in terms of its subunit and active sites composition, but shares only ca. 50% amino acid identity [22–24]. Importantly, most of the differences lie in regions remote from the FAD binding site, and would be more likely to produce changes in the interaction with the electrode, rather than in intrinsic catalytic properties. As we now report, the two enzymes show remarkably similar voltammetry, thereby supporting the proposal that the tunnel-diode effect, which limits fumarate reduction activity to a narrow region of potential, is an intrinsic property of this enzyme.

2. Materials and methods

Beef heart SQR was isolated from mitochondria by the method of Beginsky and Hatefi [25], and pure fractions of soluble SDH were obtained by resolution with perchlorate [26]. Purified *E. coli* SQR was obtained as a detergent-solubilised preparation in 0.1% Thesit (a non-ionic detergent). After removing Thesit with detergent adsorber gel (Boehringer Mannheim), the enzyme was resolved using 0.4–1.0 M perchlorate using a modification of the procedure of Davis and Hatefi [26] and precipitated at between 40 and 60% saturated ammonium sulfate. The preparation showed only the Fp and Ip subunits on SDS gels [27].

All experiments were carried out in a glove box (Vacuum Atmospheres) under an N_2 atmosphere ($O_2 < 2$ ppm). Enzyme samples were freed of residual ammonium sulfate, perchlorate, thiol, and most of the succinate by diafiltration (Amicon 8MC, YM30 membrane) against 0.1 M NaCl electrolyte/buffer solution. Supporting electrolyte consisted of 0.1 M NaCl with a mixed buffer system of 10 mM [*N*-(2-hydroxyethyl)piperazine-*N*′-(2-ethanesulfonic acid)] (HEPES), 10 mM [2-(*N*-morpholino)ethanesulfonic acid] (MES), and 10 mM [*N*-[Tris-[(hydroxymethyl)-methyl]-3-aminopropanesulfonic acid] (TAPS) all supplied by Sigma. Fumaric acid (99.5%) and succinic acid (99.5%) were supplied by Fluka. All solutions were made up with purified water (Millipore: 18 MΩ cm) and titrated to with NaOH or HCl to the desired pH at 38°C. To minimise errors in pH, ionic strength and buffer composition, each of which may distort the comparison of the two enzymes, the same buffer solutions were used to study both the beef heart and *E. coli* enzyme. Following each experiment, the pH of each cell solution was checked at the experimental temperature of 38°C. Electrochemical experiments were carried out using an AutoLab electrochemical analyser (Eco-Chemie, Utrecht, The Netherlands) equipped with GPES software and a low-current detection (ECD) module, in conjunction with a EG & G M636 electrode rotation apparatus. The all-glass, jacketted electrochemical cell and electrodes have been described previously [18]. The apparatus was housed within an earthed-Faraday cage. Prior to each experiment the pyrolytic graphite 'edge' (PGE) electrode (area 0.03 cm^2) was polished with 1 μm alumina (Buehler) and then sonicated thoroughly. A saturated calomel electrode (SCE) was used as reference electrode. The temperature of the reference electrode was checked for each set of experiments; all potentials (reported as the mean value of oxidative and reductive scans) were adjusted to the standard hydrogen electrode (SHE) scale based on a standard formula [28]. Difference voltammograms were computed by subtracting (typically) the fifth scan from the second [10], and then smoothing

the resultant trace using an in-house Fourier transformation procedure [15].

3. Results

Fig. 1a shows successive cyclic voltammograms recorded after immersing a freshly polished PGE rotating disk electrode into a pH 7.3 buffered-electrolyte solution containing *E. coli* succinate dehydrogenase (ca. 1 μM) and 1 mM succinate. The Faradaic response, an oxidative wave, is not observed in the absence of succinate; furthermore it is unaffected by the electrode rotation frequency, thus demonstrating that the current (reaction rate) is not controlled by mass transport of this substrate or dissipation of the product. As previously reported for the beef heart enzyme [10], the response develops rapidly, but decays steadily over time. If the electrode is removed from the enzyme solution, rinsed, and reinserted into a fresh succinate solution, the response persists, showing that it results from an adsorbed enzyme film. The apparent *n*-value (n_{app}) of the wave (determined from the half-height peak width (δ) of the first derivative of the current with respect to potential, as in Eq. 2 [12,15]) was consistently measured to be 1.0 ± 0.1 in the pH range 7.0–8.0, suggesting that the rate-determining step in the electrocatalysis involves the transfer of one electron [10,11].

$$n_{app} = 3.53RT/\delta F \quad (2)$$

If fumarate is present in addition to succinate, the adsorbed enzyme operates in both directions and the activities can be compared. In Fig. 1b, which shows voltammograms recorded at pH 7.2 in solutions containing 1 mM succinate and 1 mM fumarate, the most striking feature is the intense reductive current peak (at ε_{peak}) on both forward and backward scans. Again, the voltammetric response is independent of electrode rotation rate and voltage scan rate up to 50 mV s^{-1}, thereby showing that the voltammetry is at steady state. Successive cycles, decreasing in current amplitude, generate isosbestic potentials (at ε_{isos}), at which there is no net current; thus, if fumarate and succinate are at equal concentration, the average value of ε_{isos} from both scan directions (separated by up to 20 at 10 mV s^{-1}) is equal to the formal reduction

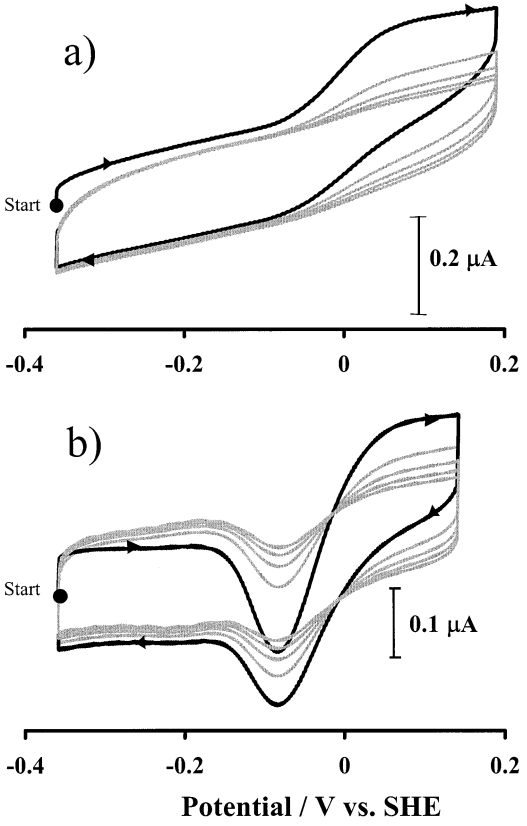

Fig. 1. Successive cyclic voltammograms observed for *E. coli* SDH films at a pyrolytic graphite 'edge' electrode in contact with solutions containing: (a) 1 mM succinate (pH 7.3); (b) 1 mM succinate+1 mM fumarate (pH 7.2). Scan rates 10 and 20 mV/s, respectively, electrode rotation rate 400 rpm, temperature 38°C. The supporting buffer/electrolyte consists of 10 mM HEPES, 10 mM MES, 10 mM TAPS, with 0.1 M NaCl. Enzyme adsorbed from ca. 1 μM concentration in solution. The first scans for a and b are shown highlighted in bold. In b, the isosbestic potential can be seen as the intersection point of the catalytic waves.

potential of the fumarate/succinate couple, (abbreviated as $\varepsilon_{F/S}$) $\varepsilon_{F/S}$, at that particular pH [10,11]. Fig. 2 compares $\varepsilon_{F/S}$ values obtained for *E. coli* SDH with those determined in experiments with the beef heart enzyme. The two data sets are very similar; $\varepsilon_{F/S}$ is ca. 0 mV at pH 7, and the pH dependence is close to the value of −62 mV expected for the $2H^+/2e^-$ reaction at 38°C [8]. The succinate and fumarate concentrations used were greater than their respective K_m values [29–31], and so no significant variation with concentration (1–20 mM) was observed.

Since reversible signals due to individual redox centres have not as yet been observed in the absence

of substrate, the coverage of electroactive enzyme molecules in these experiments must be very low (<1 pmol cm^{-2}). This is consistent with the rotation-rate independence, since substrate depletion is not expected if the electroactive sites are limited to isolated zones to which diffusion is radial [32]. In support of this statement, comparison may be made with cytochrome *c* peroxidase (yeast) [16,17], fumarate reductase (*E. coli*) [12,15,18], and flavocytochrome c_3 (*S. frigidimarina*) [19], which each adsorb to dense coverage at PGE electrodes and display well-defined non-turnover signals, addition of substrate revealing high catalytic activity with a strong rotation rate dependence. The unknown surface coverage precludes analysis of the voltammetry of SDH to give absolute rate values. However because the active coverage decreases progressively over time, and since the catalytic activity appears to be binary in nature (enzyme molecules are either fully active or completely inactive, so that partially disabled or misoriented fractions do not contribute to the waveform) it is possible to generate steady-state difference voltammograms. Assuming that the change in background current is negligible, these

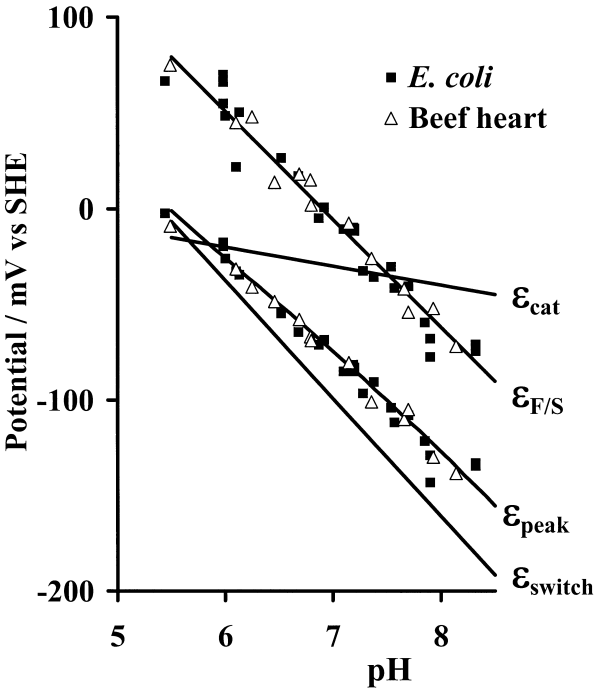

Fig. 2. Experimentally determined values of $\varepsilon_{F/S}$ and ε_{peak} as a function of pH, for SDH from *E. coli* (■) and beef heart mitochondria (△). Conditions are as described in the text. Also shown are lines indicating the modelling parameters ε_{cat} and ε_{switch} and lines showing $\varepsilon_{F/S}$ and ε_{peak} predicted by the model.

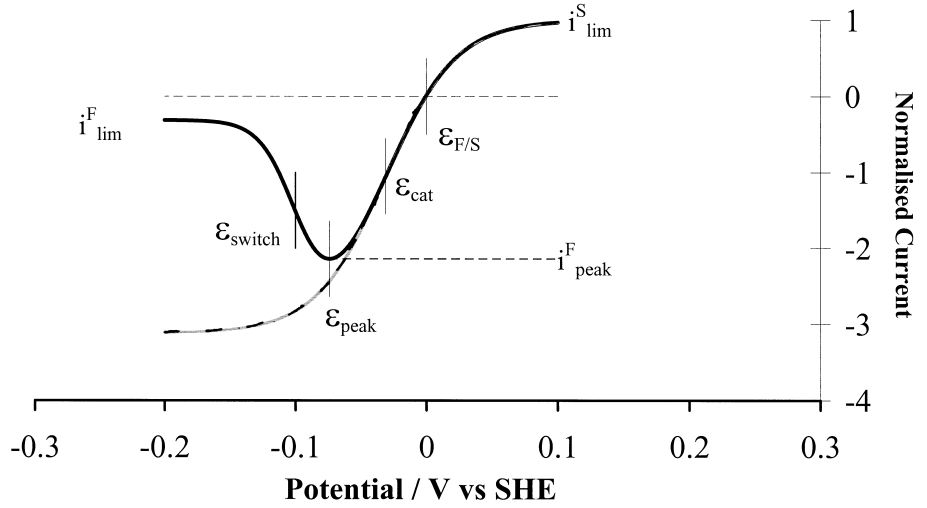

Fig. 3. An idealised difference voltammogram or catalytic profile for SDH acting on a 1:1 succinate/fumarate mixture (pH 7.0, 38°C) showing the *i–E* characteristics used to define the kinetic and thermodynamic similarities and differences between beef heart and *E. coli* enzymes. Of the experimentally measured parameters, i^{S}_{lim} reflects the rate of succinate oxidation, whereas i^{F}_{peak} and i^{F}_{lim} correspond to the rate of fumarate reduction by the more-active (high potential) and less-active (low potential) states of the enzyme, respectively. $\varepsilon_{F/S}$ is the isosbestic potential (and Nernstian potential of the substrates) and ε_{peak} is the potential of maximum fumarate reduction activity. The other two parameters are derived from simulation: ε_{switch} is the potential of the site effecting transition between the more and less active states, assigned as the FAD/FADH$_2$ potential, while ε_{cat} is the 'catalytic' potential of the enzyme, i.e. the half-height potential of the more-active state catalytic wave (shown completed, in the absence of transition to the less-active state by (- - -)).

traces reveal the variations in relative catalytic activity (fumarate reduction versus succinate oxidation) as a function of potential [10,11]. Fig. 3 shows a idealised voltammogram (pH 7.0) for *E. coli* SDH, indicating the parameters of interest: $\varepsilon_{F/S}$ and ε_{peak} are measured experimentally while ε_{cat} (the operating potential) and ε_{switch} (the potential of the tunnel-diode producing transition) are determined from the model as described previously [10,11]. Additionally we compare three activity measurements: the limiting value of the succinate oxidation current i^{S}_{lim}; the limiting fumarate reduction current at low potential i^{F}_{lim}; and the fumarate peak current i^{F}_{peak}. The absolute values of these currents are, of course, dependent on active coverage, but their ratios quantify the relative catalytic activities as functions of potential.

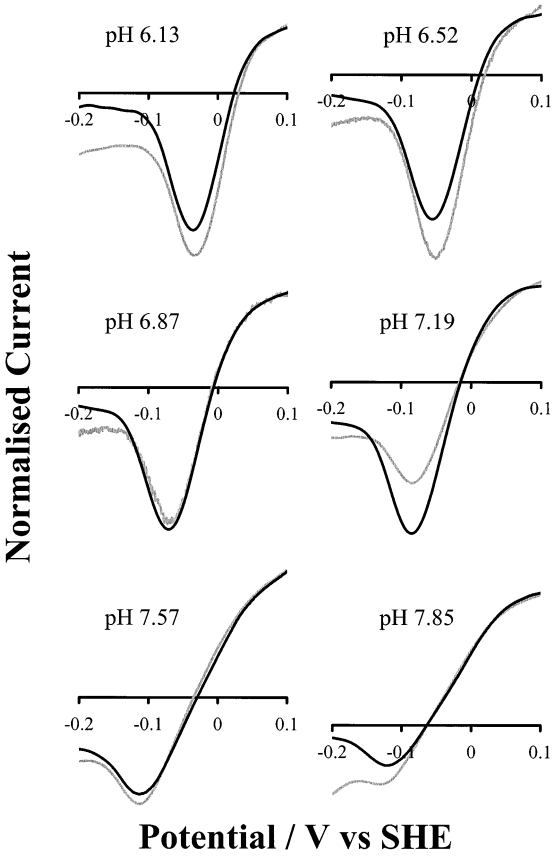

Fig. 4. Comparison of the steady-state activities of SDH from *E. coli* (black lines) and beef heart (grey lines) in solutions containing 1 mM succinate and 1 mM fumarate for a range of different pH values. Conditions: Scan rates, 10 mV s^{-1}, 38°C; and electrode rotation rates, typically 400 rpm. Supporting buffer/electrolytes contained 10 mM HEPES, 10 mM MES, 10 mM TAPS, and 0.1 M NaCl. Enzyme film adsorbed from ca. 1 μM SDH in solution. The pH values indicated refer to the *E. coli* enzyme: corresponding values for the beef heart enzyme are (parentheses), 6.13 (6.10); 6.52 (6.46); 6.87 (6.80); 7.19 (7.15); 7.57 (7.66) and 7.85 (7.93). Difference voltammograms were computed as described in the text. The data for both enzymes have been normalised with respect to equal limiting succinate oxidation activity.

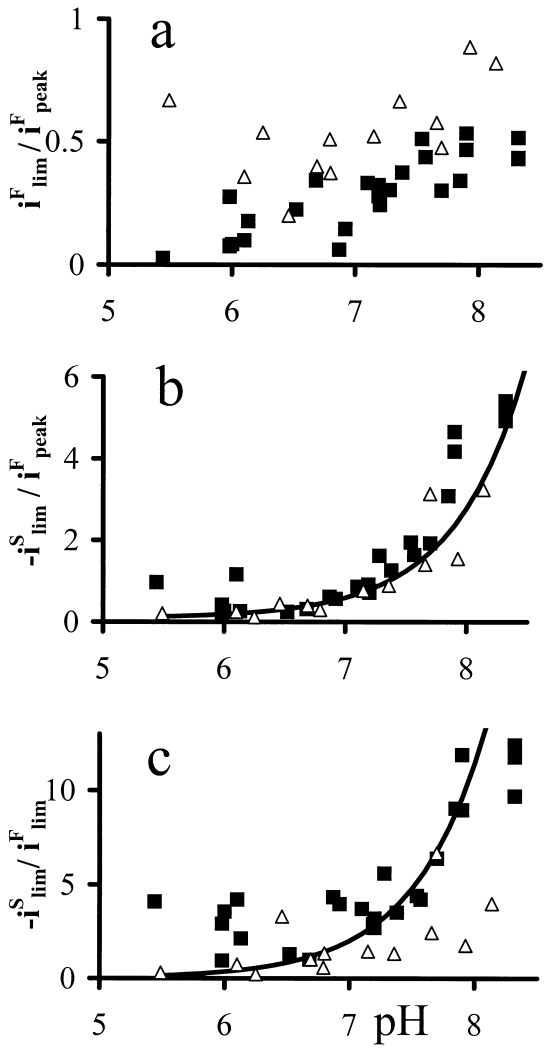

Fig. 5. Experimentally determined current ratios (a) i^{F}_{lim}/i^{F}_{peak}, (b) $-i^{S}_{lim}/i^{F}_{peak}$ and (c) $-i^{S}_{lim}/i^{F}_{lim}$ as a function of pH for SDH from *E. coli* (■) and beef heart mitochondria (△). Also shown (as solid lines) are the ratios for *E. coli* SDH predicted by the model.

Fig. 4 compares six pairs of difference voltammograms from *E. coli* and beef heart SDH recorded at very similar pH values: in order to facilitate direct comparison, voltammograms have been normalised with respect to their succinate oxidation currents. There is a good qualitative correlation between the

catalytic profiles. However, in each case, the magnitude of the limiting fumarate current for the *E. coli* SDH is lower than that observed for the beef heart enzyme. This effect is quantified more clearly by Fig. 5a, which illustrates how the current ratio i^{F}_{lim}/i^{F}_{peak} varies with pH for the two enzymes. Values of limiting fumarate currents are difficult to measure, as they are frequently complicated by background slope [10,11]; consequently, the errors are large. Nevertheless, the values for i^{F}_{lim}/i^{F}_{peak} are consistently smaller for *E. coli* SDH than for the beef heart enzyme.

The model for beef heart SDH considers a switch between a more-active and a less-active form, according to a reduction potential ε_{switch} which involves cooperative transfer of two electrons ($n_{switch} = 2$) [10,11]. As shown in Fig. 2, values of ε_{peak} measured for the beef heart and *E. coli* enzymes are equal, within experimental error, and display a pH dependence of ca. −50 mV per pH unit over the range 5.5–8.5. The simulation parameters ε_{cat} and ε_{switch} (listed in Table 1) and the relative activities of the more-active and less-active forms were each adjusted until the fit between predicted and experimental results was optimised – for the ε_{peak} potentials (Fig. 2), the three current ratios, i^{F}_{lim}/i^{F}_{peak}, $-i^{S}_{lim}/i^{F}_{peak}$, $-i^{S}_{lim}/i^{F}_{lim}$ (Fig. 5) and the normalised difference voltammograms, as shown in Fig. 6 [10,11]. As observed for beef heart SDH [10,11], the underlying catalytic waveform for the *E. coli* enzyme corresponds to a one-electron process ($n_{cat} = 1$), with a small pH dependence (ca. 10 mV per pH unit). For both enzymes, the catalytic operating potential ε_{cat} is more negative than $\varepsilon^{0'}_{F/S}$ at pH < 7.6, where the enzyme is biased towards fumarate reduction. Fig. 2 also shows how the computed reduction potential ε_{switch} for both beef heart and *E. coli* SDH (−100 ± 15 mV, pH 7.0, 38°C) decreases by 60 mV/pH unit, close to the value of 62 mV expected for a 1:1 ratio of protons and electrons. Since the switch can only be modelled satisfactorily in terms of $n_{switch} = 2$, the conclusion is that it arises from a $2H^{+}/2e^{-}$ reaction. In contrast to beef heart SDH, for which the less-active form shows ca. 30–40% activity relative to that expected of the more-active form [10], modelling of the *E. coli* enzyme requires that the less-active form exhibits only 8–20% of the activity expected of the fully active form across the pH range 5.5–8.5, i.e. there is a greater shutdown of activity at low potentials.

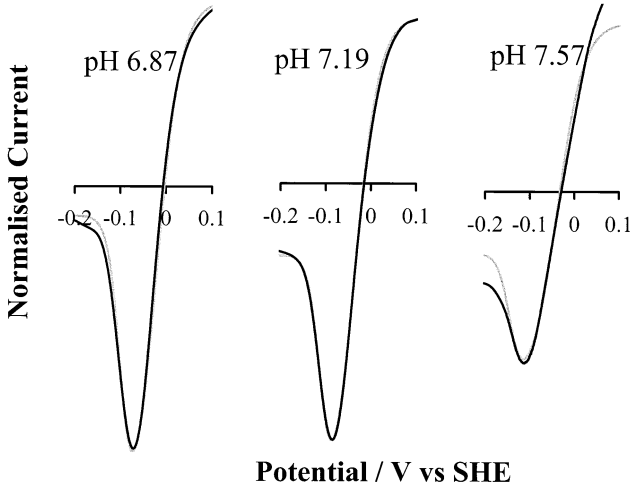

Fig. 6. Difference voltammograms (black curves) and simulation results (grey curves) obtained for *E. coli* SDH. The experimental results have been modified by background subtraction and normalisation as described in the text. The parameters used in the model correspond to those presented in Fig. 4 and discussed in the text. The data are normalised with respect to equal limiting succinate oxidation activity.

4. Discussion

Protein-film cyclic voltammetry experiments reveal that when adsorbed as a film at an electrode surface, succinate dehydrogenase from *E. coli* catalyses the interconversion of fumarate and succinate at reversible potentials, with relative catalytic activities showing very similar potential and pH dependencies to those reported previously for the beef heart enzyme [10,11]. The voltammetry is controlled by the enzyme, with no evidence for kinetic limitations arising either from mass-transport of substrate/product (between bulk solution and adsorbed enzyme), or from sluggish interfacial electron transfer (between adsorbed enzyme and the electrode surface). Consequently, the observed cyclic voltammograms provide a direct readout of the enzyme's catalytic activity as a continuous function of potential. As shown in Table 1, the catalytic energetics of beef heart and *E. coli* succinate dehydrogenases, derived from the voltammetry, are virtually identical. The clearly observed bidirectional nature of the electrochemistry, the fact that both *E. coli* and beef heart SDH show an ener-

Fp Subunit

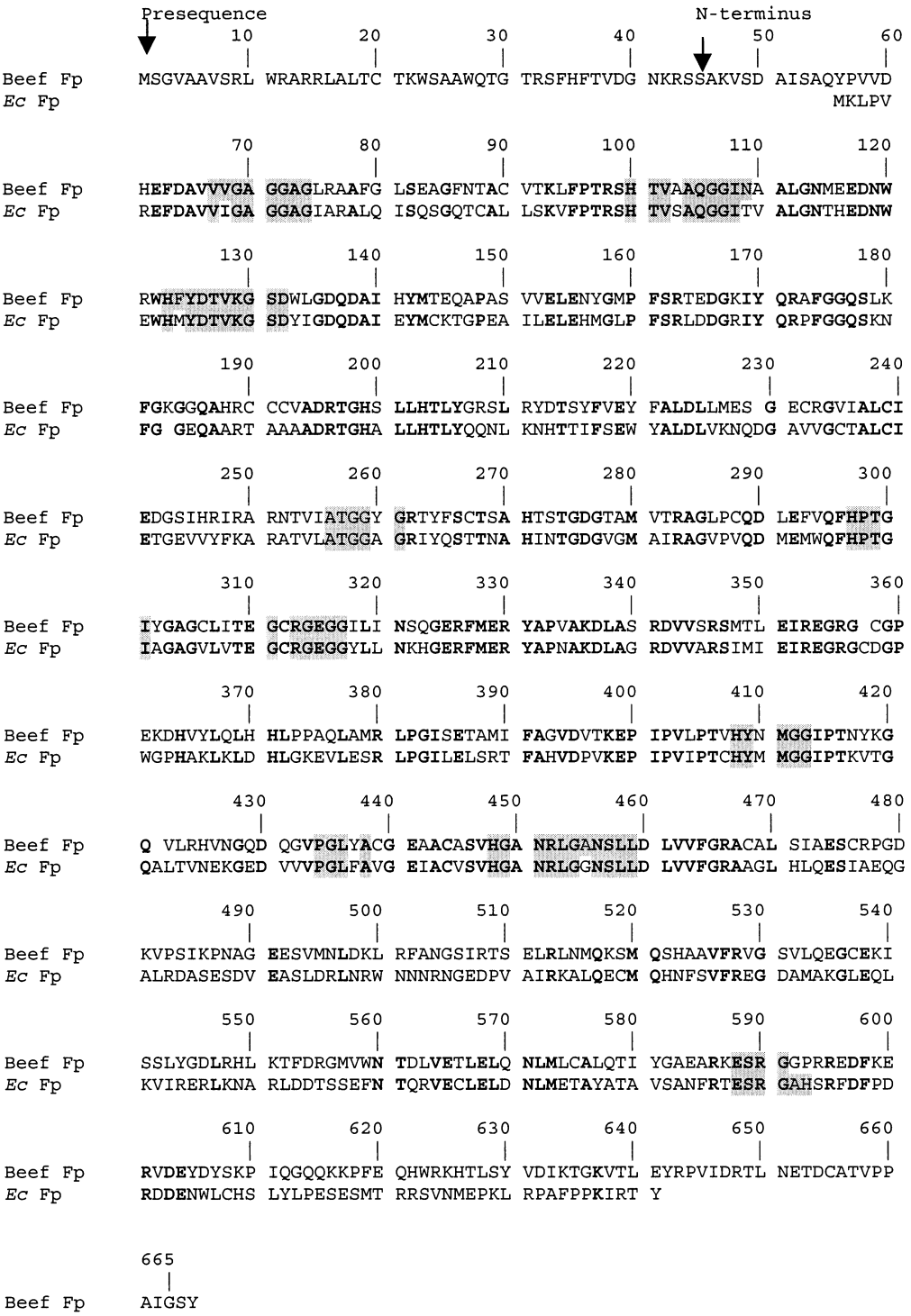
Presequence
N-terminus
Beef Fp MSGVAAVSRL WRARRLALTC TKWSAAWQTG TRSFHFTVDG NKRSSAKVSD AISAQYPVVD
Ec Fp MKLPV
Beef Fp HEFDAVVVGA GGAGLRAAFG LSEAGFNTAC VTKLFPTRSH TVAAQGGINA ALGNMEEDNW
Ec Fp REFDAVVIGA GGAGIARALQ ISQSGQTCAL LSKVFPTRSH TVSAQGGITV ALGNTHEDNW
Beef Fp RWHFYDTVKG SDWLGDQDAI HYMTEQAPAS VVELENYGMP FSRTEDGKIY QRAFGGQSLK
Ec Fp EWHMYDTVKG SDYIGDQDAI EYMCKTGPEA ILELEHMGLP FSRLDDGRIY QRPFGGQSKN
Beef Fp FGKGGQAHRC CCVADRTGHS LLHTLYGRSL RYDTSYFVEY FALDLLMES G ECRGVIALCI
Ec Fp FG GEQAART AAAADRTGHA LLHTLYQQNL KNHTTIFSEW YALDLVKNQDG AVVGCTALCI
Beef Fp EDGSIHRIRA RNTVIATGGY GRTYFSCTSA HTSTGDGTAM VTRAGLPCQD LEFVQFHPTG
Ec Fp ETGEVVYFKA RATVLATGGA GRIYQSTTNA HINTGDGVGM AIRAGVPVQD MEMWQFHPTG
Beef Fp IYGAGCLITE GCRGEGGILI NSQGERFMER YAPVAKDLAS RDVVSRSMTL EIREGRG CGP
Ec Fp IAGAGVLVTE GCRGEGGYLL NKHGERFMER YAPNAKDLAG RDVVARSIMI EIREGRGCDGP
Beef Fp EKDHVYLQLH HLPPAQLAMR LPGISETAMI FAGVDVTKEP IPVLPTVHYN MGGIPTNYKG
Ec Fp WGPHAKLKLD HLGKEVLESR LPGILELSRT FAHVDPVKEP IPVIPTCHYM MGGIPTKVTG
Beef Fp Q VLRHVNGQD QGVPGLYACG EAACASVHGA NRLGANSLLD LVVFGRACAL SIAESCRPGD
Ec Fp QALTVNEKGED VVVPGLFAVG EIACVSVHGA NRLGGNSLLD LVVFGRAAGL HLQESIAEQG
Beef Fp KVPSIKPNAG EESVMNLDKL RFANGSIRTS ELRLNMQKSM QSHAAVFRVG SVLQEGCEKI
Ec Fp ALRDASESDV EASLDRLNRW NNNRNGEDPV AIRKALQECM QHNFSVFREG DAMAKGLEQL
Beef Fp SSLYGDLRHL KTFDRGMVWN TDLVETLELQ NLMLCALQTI YGAEARKESR GGPRREDFKE
Ec Fp KVIRERLKNA RLDDTSSEFN TQRVECLELD NLMETAYATA VSANFRTESR GAHSRFDFPD
Beef Fp RVDEYDYSKP IQGQQKKPFE QHWRKHTLSY VDIKTGKVTL EYRPVIDRTL NETDCATVPP
Ec Fp RDDENWLCHS LYLPESESMT RRSVNMEPKL RPAFPPKIRT Y
665
Beef Fp AIGSY

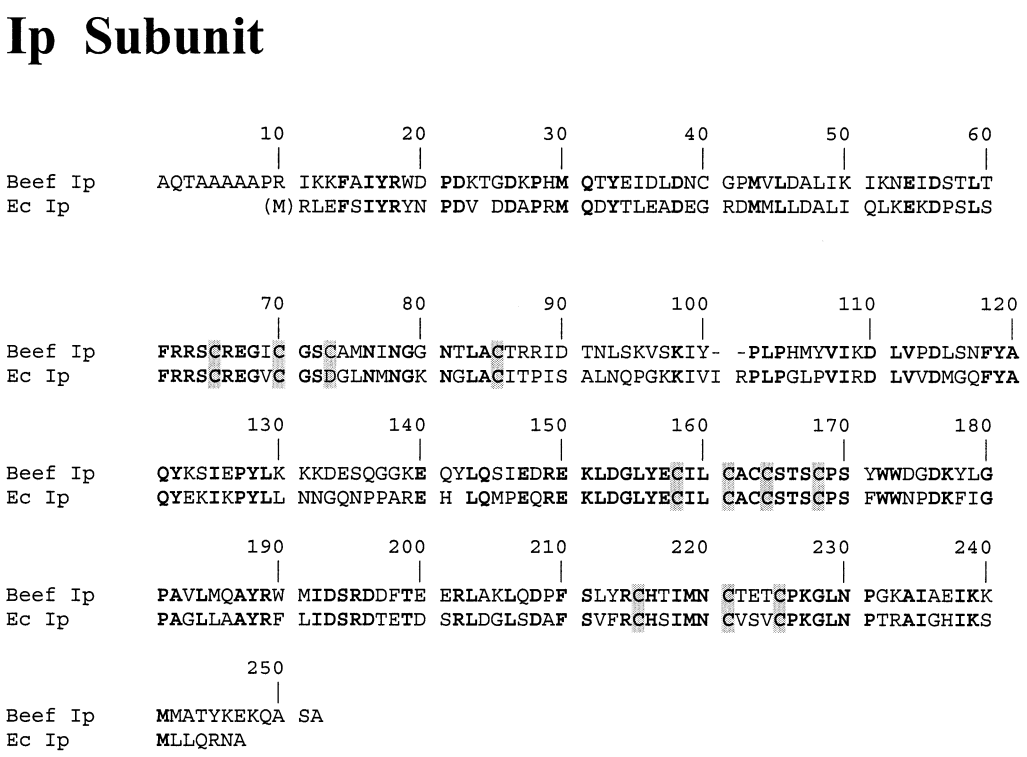

Fig. 7. Aligned amino acid sequences for the Fp and Ip subunits of beef heart and *E. coli* SDH [22–24,36,37]. The sequence homology is ca. 50% for both subunits; conserved residues are marked in bold. The shaded regions correspond to binding domains for flavin, nucleotide and substrate in the Fp sequences (with H100 being the site of covalent linkage of the FAD cofactor), and iron–sulfur clusters in the Ip sequences. The N-terminus of the mature Fp polypeptide (i.e. after cleavage of the leader sequence) is marked as residue S45. The beef Ip presequence is not shown.

getic bias towards fumarate reduction at pH values less than 7.6 (intersection of the lines for ε_{cat} and $\varepsilon_{F/S}$ in the pH-dependence graph of Fig. 2) [10,11], and the modest difference (ca. 70–110 mV) between $\varepsilon_{F/S}$ and the ubiquinone/ubiquinol reduction potential [33] all suggest that this part of the citric acid cycle is quite reversible. By contrast, even below pH 7.6, conventional solution-phase measurements of the catalytic activities of succinate dehydrogenases have usually shown lower activity for fumarate reduction compared to succinate oxidation [31,34,35].

For *E. coli* SDH, as was the case with the beef heart enzyme, fumarate reduction activity decreases abruptly as the potential is lowered, i.e. the enzyme displays a 'tunnel-diode' effect. As discussed previously, the more-active and less-active states of the enzyme might arise from the adoption of slightly different conformations depending on whether the FAD is oxidised or reduced [10]. Since the lifetimes of FAD oxidation states during catalysis are very short, conformational interconversions depend upon the steady-state level that can be maintained by the applied potential. The reduction potential of the $FAD/FADH_2$ couple has not been reported for the *E. coli* enzyme; however, the close agreement between the reduction potentials of the $2H^+/2e^-$ redox switches in the two enzymes suggests that they have the same origin.

The results obtained with *E. coli* SDH provide further evidence that the tunnel diode behaviour seen in the voltammetry for beef heart SDH is an intrinsic property of the enzyme and does not arise from a potential-dependence of the coupling with the electrode. As reported earlier, the latter must be considered unlikely, as the tunnel-diode behaviour occurs for beef heart SDH with the same fumarate reduction peak potentials at both bare gold and graphite electrodes [21]. The effect is seen also at a tin-doped indium oxide electrode (unpublished observations), and is consistently inferred from experiments carried out with redox mediating dyes for a range of SQR samples in solution [21].

Fig. 7 compares the primary structures of SDHs from beef heart [22–24] and *E. coli* [36,37], and shows that the flavoprotein and iron–sulfur subunits each share ca. 50% amino acid identity between the two sources. This identity is located primarily around binding regions believed to be associated with FAD and the substrate in the larger subunit, and the iron–sulfur clusters in the smaller subunit. Using the ExPASy isoelectric point (p*I*) calculation program [38–41] (which neglects the effects of protein conformation and the presence of the FAD and iron–sulfur centres) we estimated the p*I* values of mature beef heart and *E. coli* SDH to be 6.7 and 5.9, respectively, thereby predicting different overall charges for the two proteins. Were protein–electrode interactions to be the origin of the tunnel-diode effect, such a difference in electrostatics might be expected to cause a significant shift in the characteristic potentials of the voltammograms. The fact that both beef heart and *E. coli* SDH display the tunnel-diode effect with the same fumarate reduction peak potentials argues strongly that potential-dependent interfacial processes are not responsible for the observed voltammetry. The tunnel diode effect must therefore result from intrinsic properties that are conserved between the two enzymes.

The specific physiological significance of the tunnel-diode effect is unclear, partly because the enzyme studied is the soluble form, and not the membrane-bound SQR complex. Succinate dehydrogenases are generally expressed in vivo under aerobic conditions, and it is difficult to see how the switch might be accessed, unless the local conditions caused, perhaps transiently, the reduction potential to stray to more negative values, in which case, the fumarate reductase activity would be shut down, the effect acting as a 'rachet' [42]. Nevertheless, it is clear that SDH, and possibly the complete SQR complex, is a very effective fumarate reductase within the narrow thermodynamic region between the fumarate reduction potential and ε_{switch}. On a more general note, the idea that the catalytic activities of redox enzymes may show an electrochemical potential-dependence (cf. pH dependence) has not been well explored, but may well represent an important aspect of metabolic regulation.

Acknowledgements

We thank Dr. Dirk Heering for developing useful data analysis software and for many valuable discussions, and Dr. Gary Cecchini for the very generous gift of *E. coli* SQR. This work has been funded by the UK Engineering and Physical Sciences Research Council, The Wellcome Trust (Grant 042109), and the US National Institutes of Health (USPHS Program HL-16251).

References

[1] L. Hederstedt, T. Ohnishi, in: L. Ernster (Ed.), Molecular Mechanisms in Bioenergetics, Elsevier, New York, 1992, pp. 163–198.
[2] B.A.C. Ackrell, M.K. Johnson, R.P. Gunsalus, G. Cecchini, in: F. Muller (Ed.), Chemistry and Biochemistry of Flavoenzymes, CRC, Boca Raton, FL, 1992.
[3] C. Hägerhäll, Biochim. Biophys. Acta 1320 (1997) 107–141.
[4] T. Ohnishi, T.E. King, J.C. Salerno, H. Blum, J.R. Bowyer, T. Maida, J. Biol. Chem. 256 (1981) 5577–5582.
[5] T. Ohnishi, J.C. Salerno, D.B. Winter, J. Lim, C.-A. Yu, L. Yu, T.E. King, J. Biol. Chem. 251 (1976) 2094–2104.
[6] T. Ohnishi, J. Lim, D.B. Winter, T.E. King, J. Biol. Chem. 251 (1976) 2105–2109.
[7] C. Condon, R. Cammack, D.S. Patil, P. Owen, J. Biol. Chem. 260 (1985) 9427–9434.
[8] W.M. Clark, Oxidation–Reduction Potentials of Organic Systems, Williams and Wilkins, Baltimore, MD, 1960.
[9] A. Sucheta, B.A.C. Ackrell, B. Cochran, F.A. Armstrong, Nature 356 (1992) 361–362.
[10] J. Hirst, A. Sucheta, B.A.C. Ackrell, F.A. Armstrong, J. Am. Chem. Soc. 118 (1996) 5031–5038.
[11] J. Hirst, B.A.C. Ackrell, F.A. Armstrong, J. Am. Chem. Soc. 119 (1997) 7434–7439.
[12] H.A. Heering, J. Hirst, F.A. Armstrong, J. Phys. Chem. B. 102 (1998) 6889–6902.
[13] F.A. Armstrong, H.A. Heering, J. Hirst, Chem. Soc. Rev. 26 (1997) 169.
[14] F.A. Armstrong, in: G. Lenza, G. Milazzo (Eds.), Bioelectrochemistry of Biomacromolecules, Birkhauser, Basle, 1997, pp. 205–255.
[15] H.A. Heering, J. Weiner, F.A. Armstrong, J. Am. Chem. Soc. 119 (1997) 11628–11638.
[16] M.S. Mondal, H.A. Fuller, F.A. Armstrong, J. Am. Chem. Soc. 118 (1996) 263.
[17] M.S. Mondal, D.B. Goodin, F.A. Armstrong, J. Am. Chem. Soc. 120 (1998) 6270–6276.
[18] A. Sucheta, R. Cammack, J. Weiner, F.A. Armstrong, Biochemistry 32 (1993) 5455–5465.

[19] K. Turner, M.K. Doherty, H.A. Heering, F.A. Armstrong, G.A. Reid, S.K. Chapman, Biochemistry 38 (1999) 3302–3309.
[20] E. Maklashina, D.K. Berthold, G. Cecchini, J. Bacteriol. 180 (1998) 5989–5996.
[21] B.A.C. Ackrell, F.A. Armstrong, B. Cochran, A. Sucheta, T. Yu, FEBS Lett. 326 (1993) 92–94.
[22] M.A. Birch-Machin, L. Farnsworth, B.A.C. Ackrell, B. Cochran, S. Jackson, L.A. Bindoff, A. Aitken, A.G. Diamond, D.M. Turnbull, J. Biol. Chem. 267 (1992) 11553–11558.
[23] A.A.M. Morris, L. Farnsworth, B.A.C. Ackrell, D.M. Turnbull, Biochim. Biophys. Acta 1185 (1994) 125–128.
[24] Y. Yao, S. Wakabayayashi, S. Matsuda, H. Matsubara, L. Yu, C.-A. Yu, in: H. Matsubara et al. (Eds.), Iron–Sulfur Protein Research, Japan Sci. Soc. Press, Tokyo/Springer-Verlag, Berlin, 1986, pp. 240–244.
[25] M.L. Beginsky, Y. Hatefi, J. Biol. Chem. 244 (1969) 5313–5319.
[26] K.A. Davis, Y. Hatefi, Biochemistry 10 (1971) 2509–2516.
[27] U.K. Laemmli, Nature 227 (1970) 680–685.
[28] A.J. Bard, L.R. Faulkner, Electrochemical Methods, Fundamentals and Applications, Wiley, New York, 1980.
[29] K. Kita, C.R.T. Vibat, S. Meinhardt, J.R. Guest, R.B. Gennis, J. Biol. Chem. 264 (1989) 2672–2677.
[30] P.R. Tushurashvili, E.V. Gavrikova, A.N. Ledenev, A.D. Vinogradov, Biochim. Biophys. Acta 809 (1985) 145–149.
[31] V.G. Grivennikova, E.V. Gavrikova, A.A. Timoshin, A.D. Vinogradov, Biochim. Biophys. Acta 1140 (1993) 282–292.
[32] A.M. Bond, Analyst 118 (1993) 973–978.
[33] J.C. Salerno, T. Ohnishi, Biochem. J. 192 (1980) 769–781.
[34] S.B. Vik, Y. Hatefi, Proc. Natl. Acad. Sci. USA 78 (1981) 6749.
[35] T.P. Singer, in: T.E. King, H.S. Mason, M. Morrison (Eds.), International Symposium on Oxidases and Related Redox Systems (1), J. Wiley and Sons, New York, 1965, pp. 448-481.
[36] M.G. Darlison, J.R. Guest, Biochem. J. 223 (1984) 507–517.
[37] D. Wood, M.G. Farlison, R.J. Wilde, J.R. Guest, Biochem. J. 222 (1984) 519–534.
[38] http://www.exPASy.ch/ch2d/pi_tool.html.
[39] B. Bjellqvist, G.J. Hughes, C. Pasquali, N. Paquet, F. Ravier, J.-C. Sanchez, S. Frutiger, D.F. Hochtstrasser, Electrophoresis 14 (1993) 1023–1031.
[40] B. Bjellqvist, B. Basse, E. Olsen, J.E. Celis, Electrophoresis 15 (1994) 529–539.
[41] M.R. Wilkins, E. Gasteiger, A. Bairoch, J.-C. Sanchez, K.L. Williams, R.D. Appel, D.F. Hochstrasser, in: A.J. Link (Ed.), 2-D Proteome Analysis Protocols, Humana Press, NJ, 1998.
[42] R. Cammack, in: H. Baltscheffsky (Ed.), Origin and Evolution of Biological Energy Conservation, Wiley-VCH, New York, 1996, pp. 43–70.